Figure S1. a) Location of Lettosuo, Tammela in Finland, b) Location of chambers (blue squares), water level wells (brown starts), measurement cabin (gray circle) and the Eddy Covariance tower (red circle).
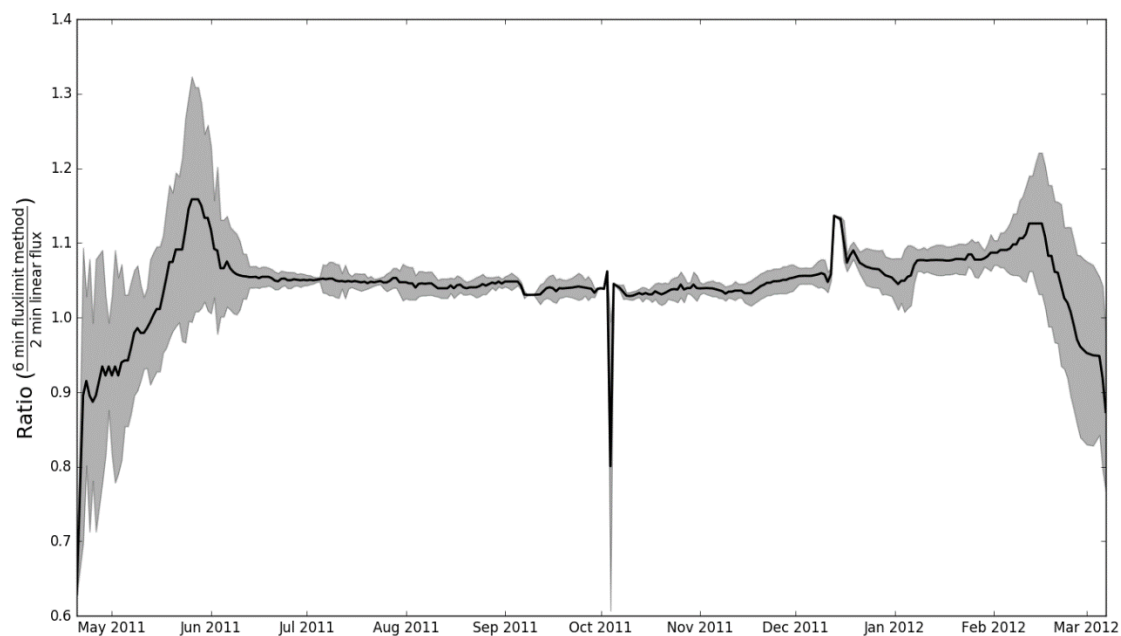

Figure S2. Smoothed correction factor (2-week moving median) for converting 2-min fluxes to the 6-min closure time. Shading shows the median absolute deviation while assuming normal distribution of the values.
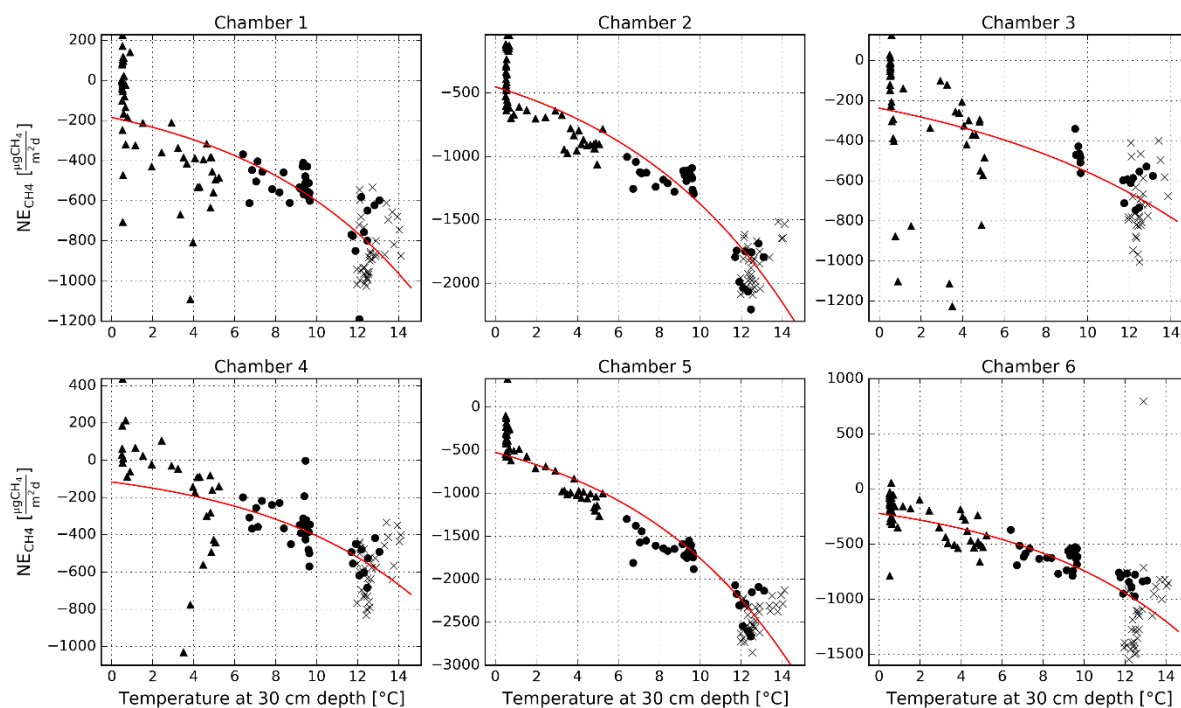
Figure S3. Daily CH₄ exchange plotted against soil temperature at 30 cm in different chambers for spring (April and May) (triangles), for the first half of the summer (1 June to 15 July) (circles) and for the second half of the summer (16 July to 31 August) (crosses) in 2011. Red curve denotes the exponential fitting (Eq. 2) to the data.
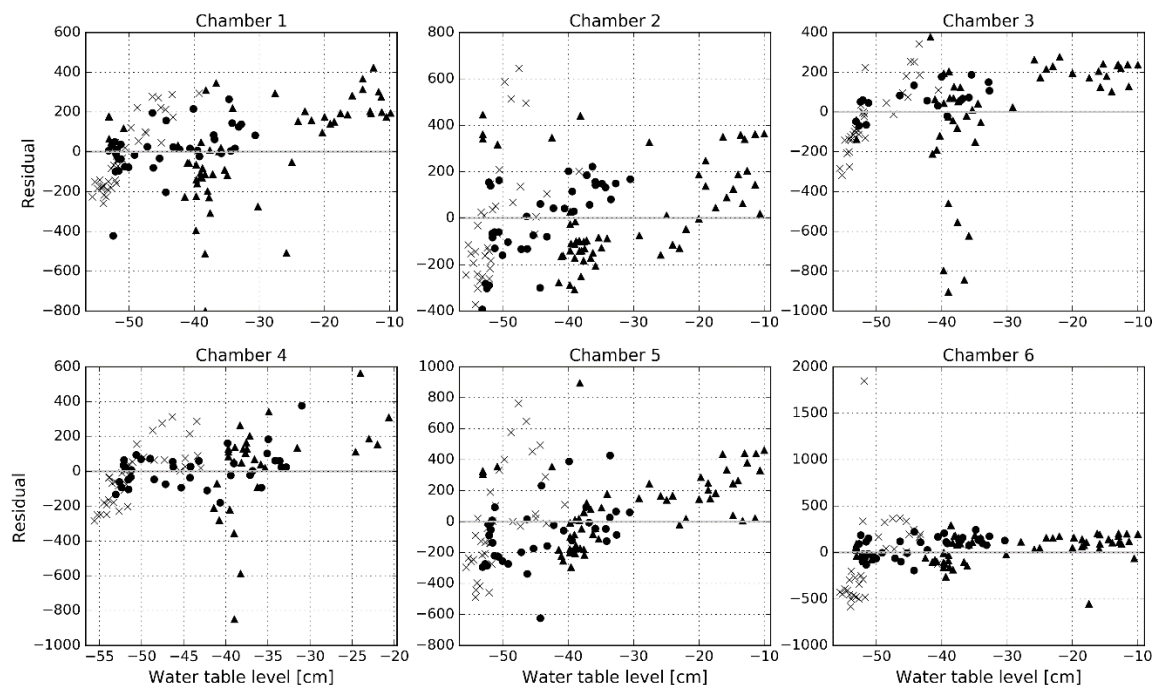

Figure S4. Residuals of the exponential fitting in Fig S3 against water table level.
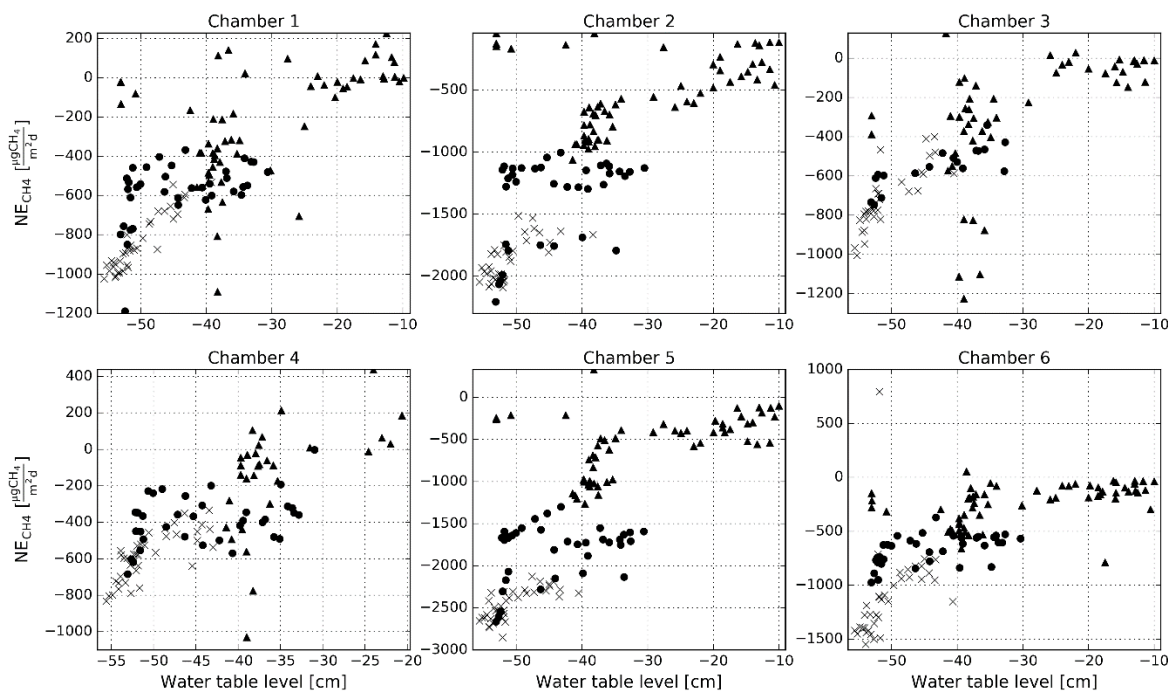
Figure S5. Daily CH₄ exchange against water table level (the same flux data as in Figures S3 and S4).
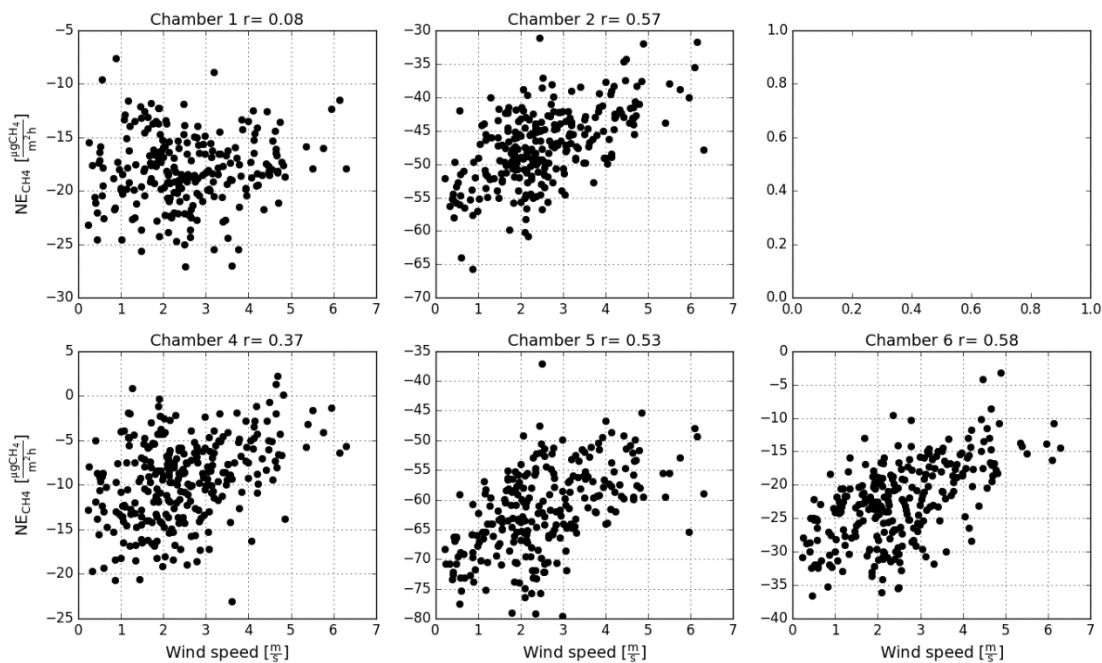

Figure S6. Hourly CH₄ fluxes against the wind speed measured above the canopy in 1-15 June 2011. Diurnal variation in CH₄ fluxes was recorded in chambers #2, #5 and #6. r in the title shows the Pearson correlation for the data.
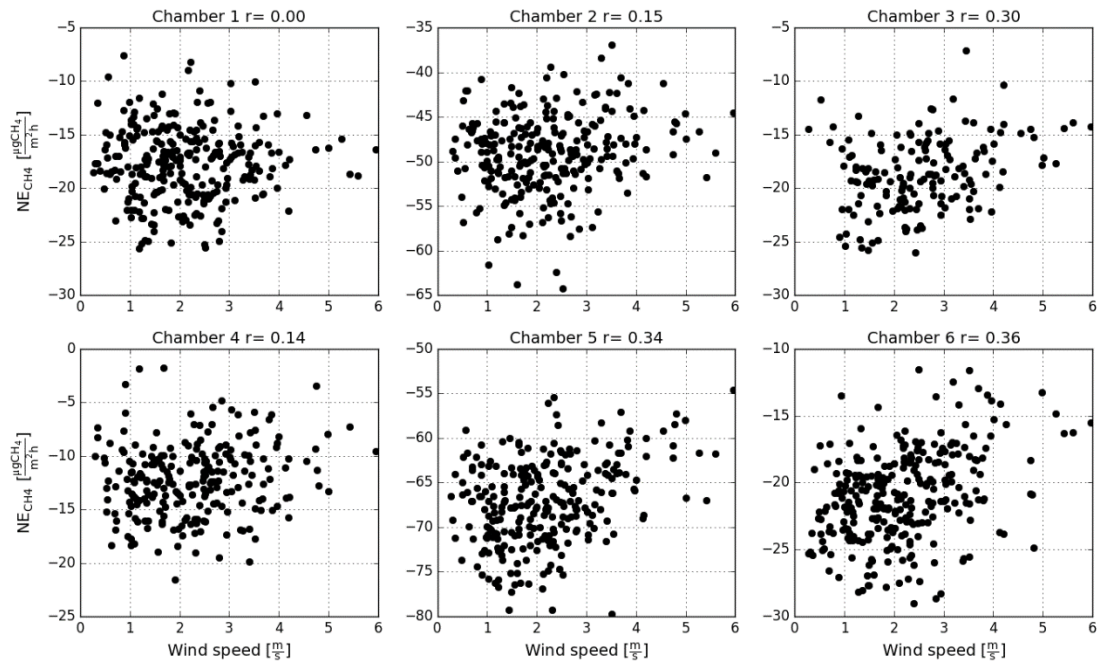
Figure S7. Hourly CH$_4$ fluxes against the wind speed measured above the canopy in 16-30 June 2011. Diurnal variation in CH$_4$ fluxes was recorded in chamber #6. r in the title shows the Pearson correlation for the data.
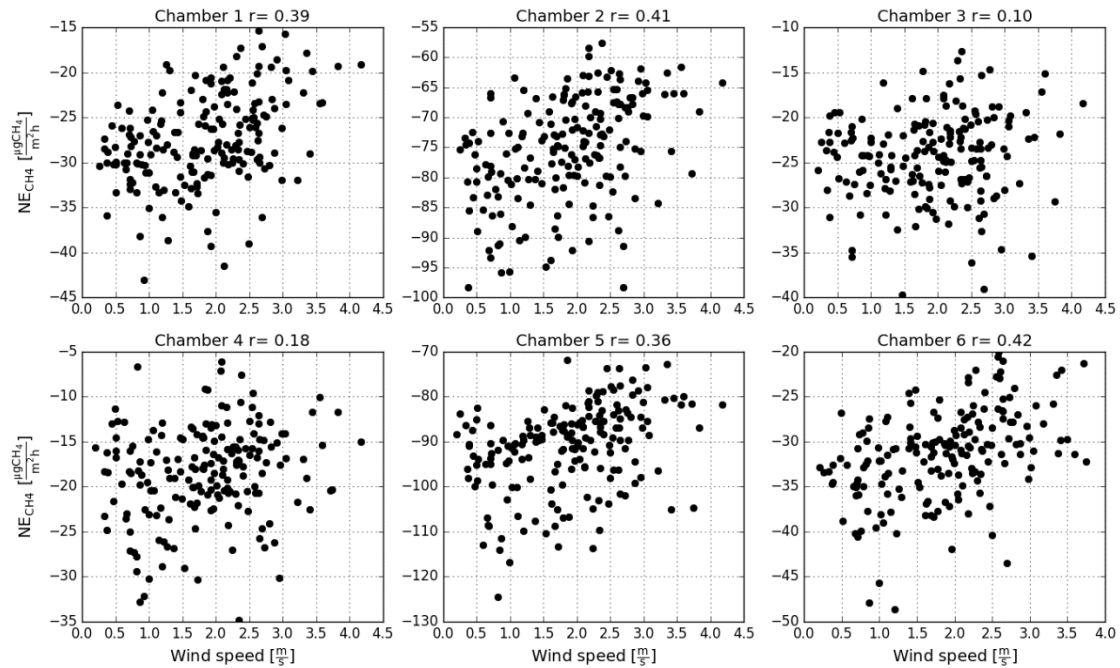

Figure S8. Hourly CH$_4$ fluxes against the wind speed measured above the canopy in 1-15 July 2011. No significant diurnal variation in CH$_4$ fluxes was recorded. r in the title shows the Pearson correlation for the data.
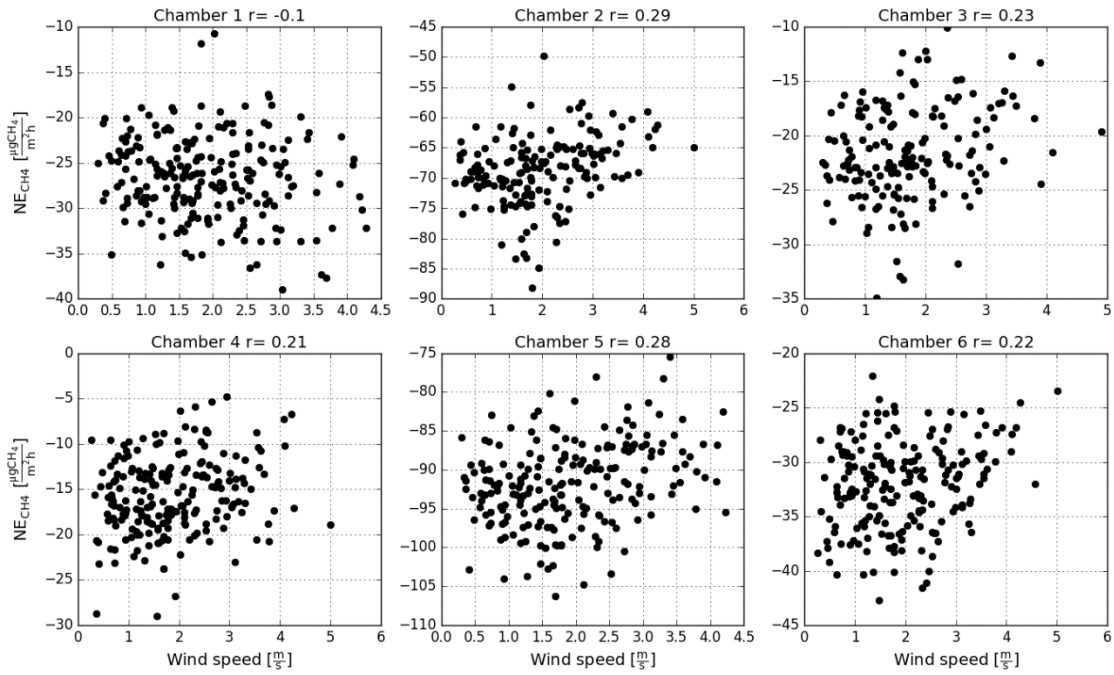
Figure S9. Hourly CH₄ fluxes against the wind speed measured above the canopy in 16-31 July 2011. Diurnal variation in CH₄ fluxes was recorded in chambers #2 and #6. r in the title shows the Pearson correlation for the data.
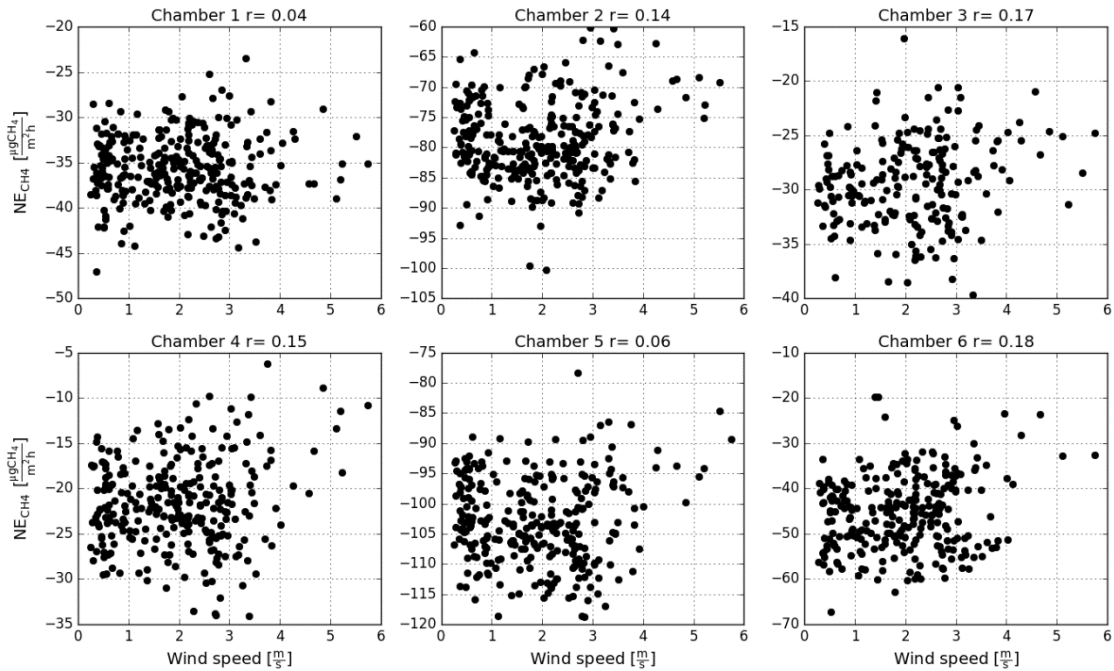

Figure S10. Hourly CH₄ fluxes against the wind speed measured above the canopy in 1-15 August 2011. Diurnal variation in CH₄ fluxes was recorded in chamber #2. r in the title shows the Pearson correlation for the data.
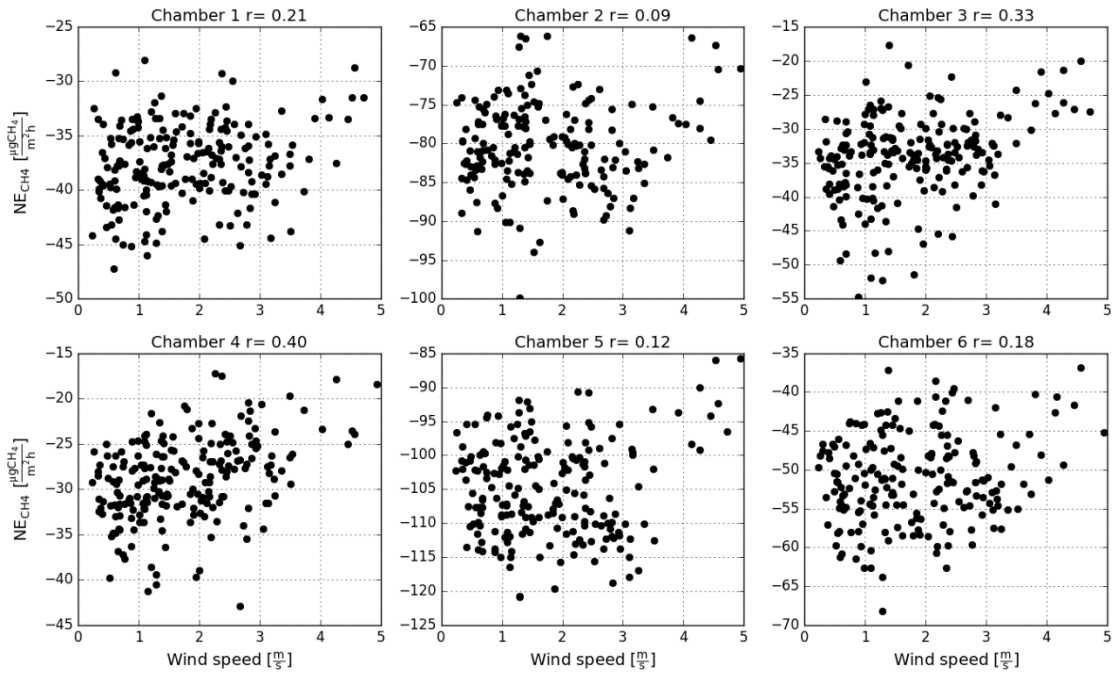
Figure S11. Hourly CH₄ fluxes against the wind speed measured above the canopy in 16-31 August 2011. Diurnal variation in CH₄ fluxes was recorded in chamber #1. r in the title shows the Pearson correlation for the data.
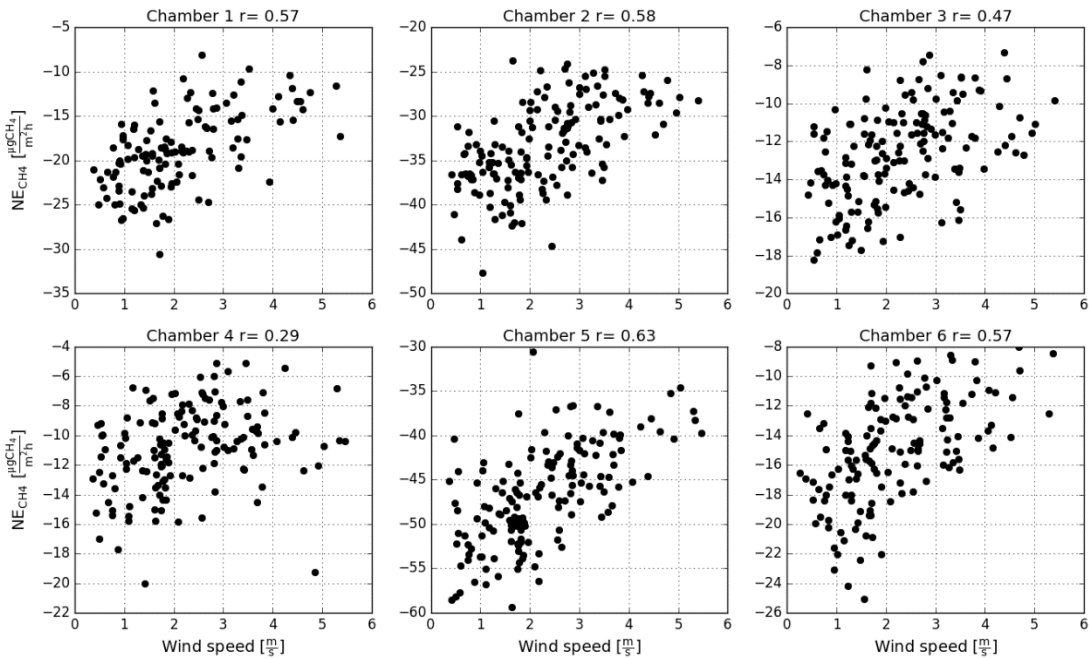

Figure S12. Hourly CH₄ fluxes against the wind speed measured above the canopy in 1-15 June 2012. Diurnal variation in CH₄ fluxes was recorded in all the chambers. r in the title shows the Pearson correlation for the data.
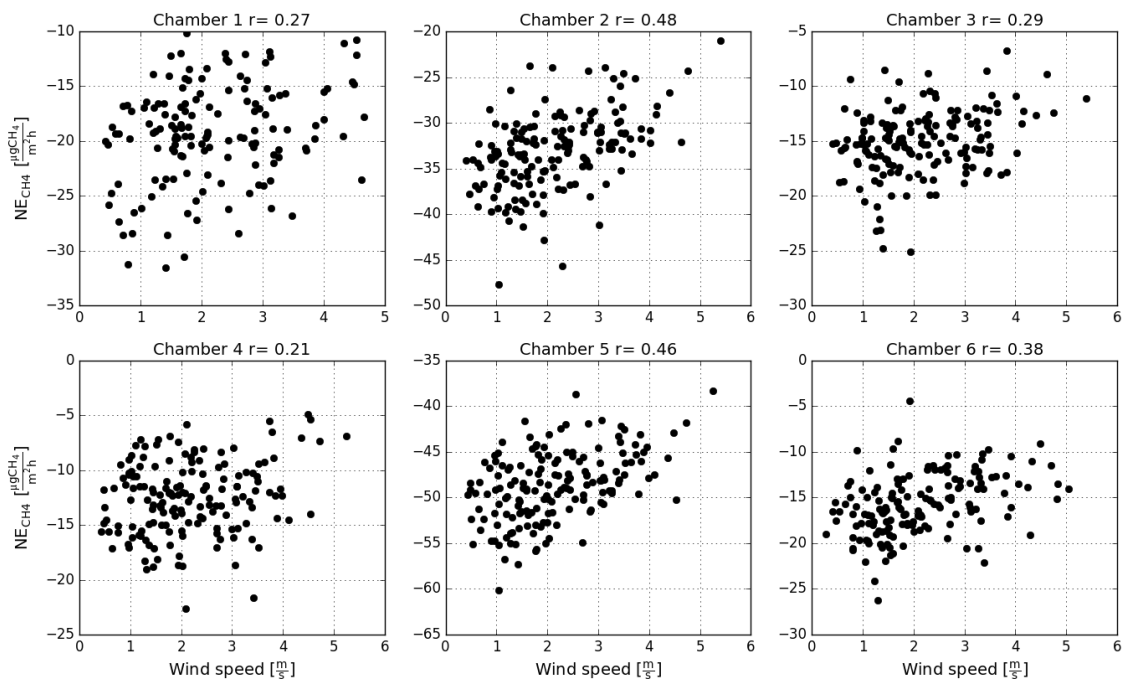
Figure S13. Hourly CH₄ fluxes against the wind speed measured above the canopy in 16-30 June 2012. Diurnal variation in CH₄ fluxes was recorded in chamber #2. r in the title shows the Pearson correlation for the data.
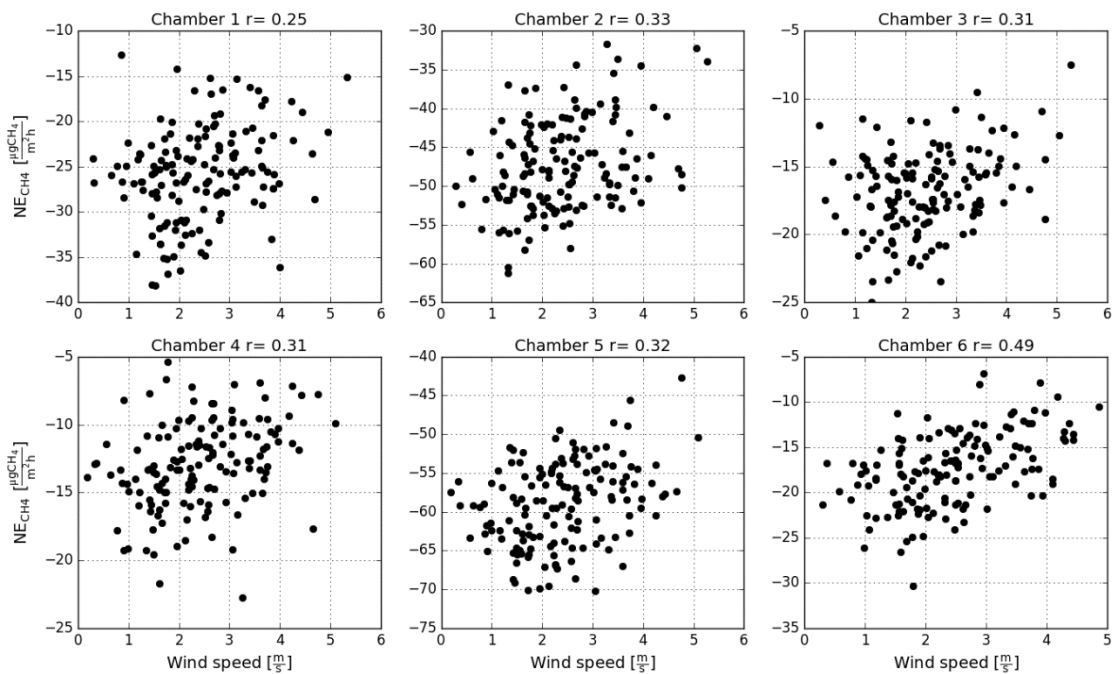

Figure S14. Hourly CH₄ fluxes against the wind speed measured above the canopy in 1-15 July 2012. Diurnal variation in CH₄ fluxes was recorded in chamber #2 and #6. r in the title shows the Pearson correlation for the data.
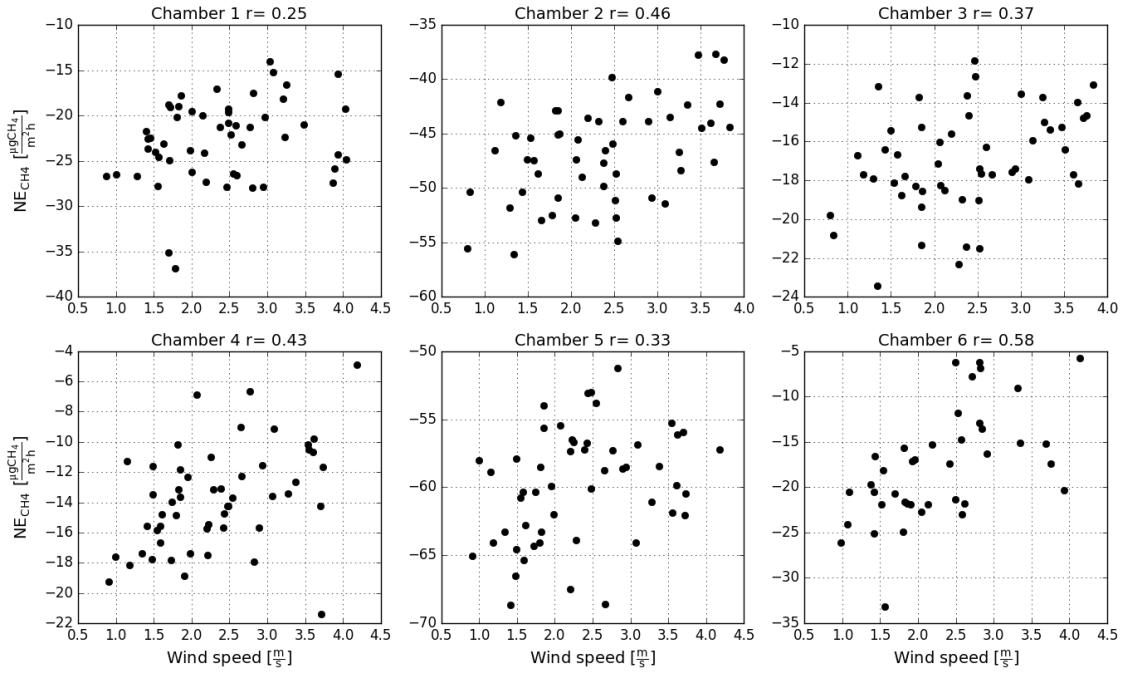
Figure S15. Hourly CH₄ fluxes against the wind speed measured above the canopy in 16-31 July 2012. No significant diurnal variation in CH₄ fluxes was recorded. r in the title shows the Pearson correlation for the data.
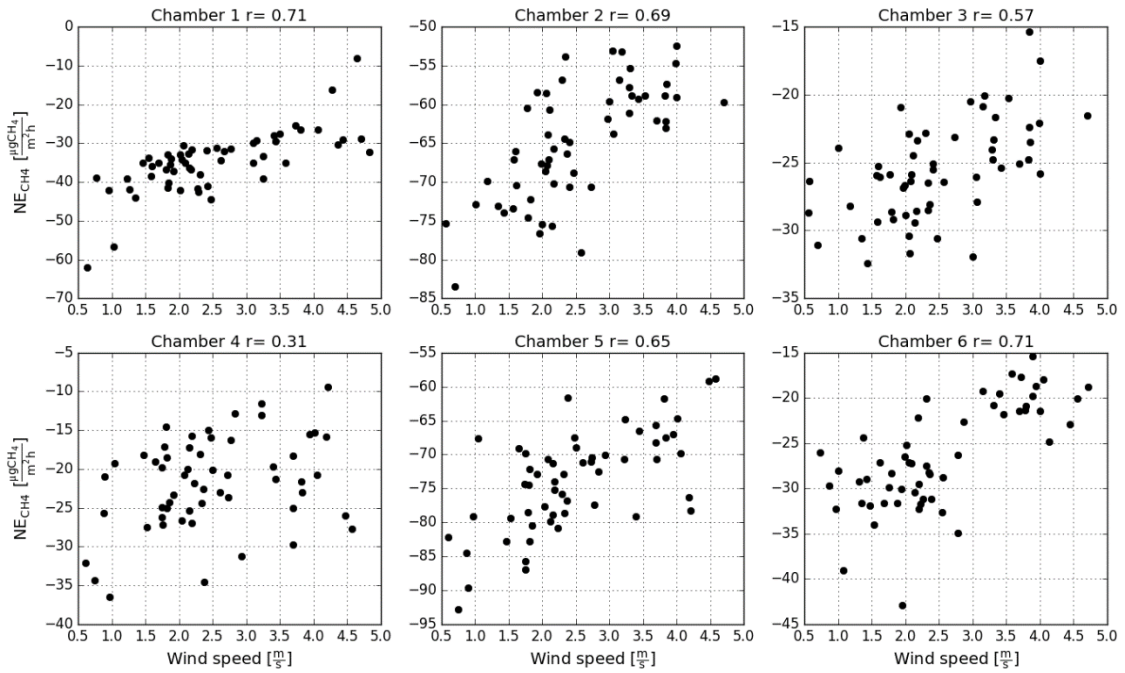

Figure S16. Hourly CH₄ fluxes against the wind speed measured above the canopy in 1-15 August 2012. No significant diurnal variation in CH₄ fluxes was recorded. r in the title shows the Pearson correlation for the data.
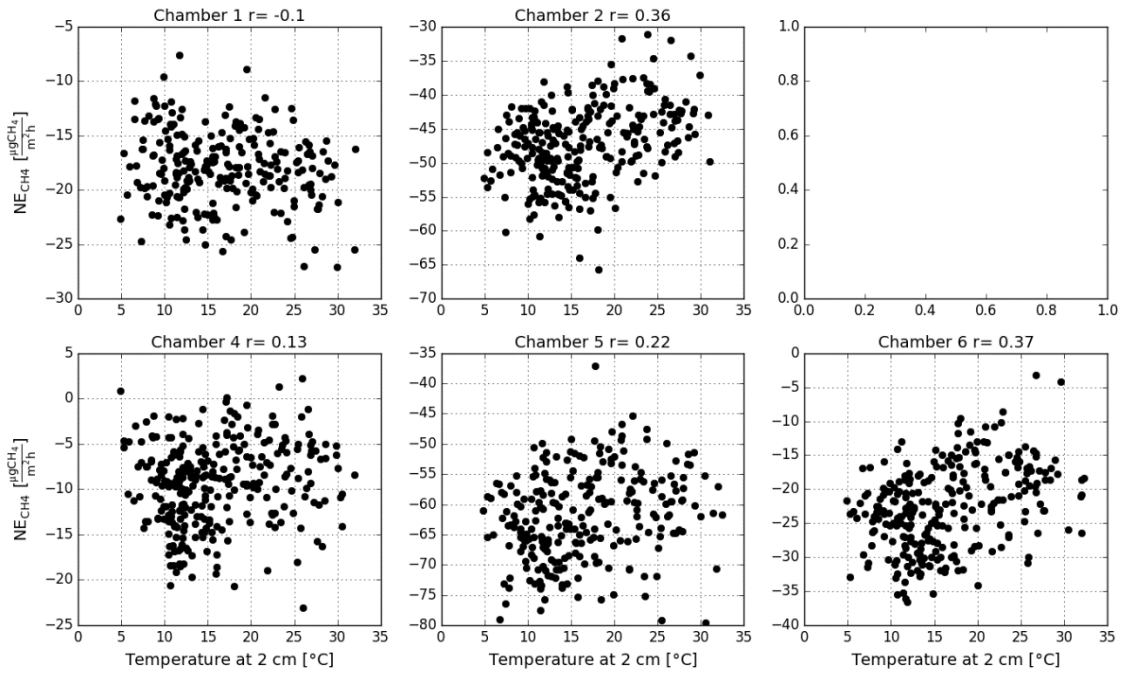
Figure S17. Hourly CH₄ fluxes against the soil temperature at 2 cm depth in 1-15 June 2011. Diurnal variation in CH₄ fluxes was recorded in chambers #2, #5 and #6. r in the title shows the Pearson correlation for the data.
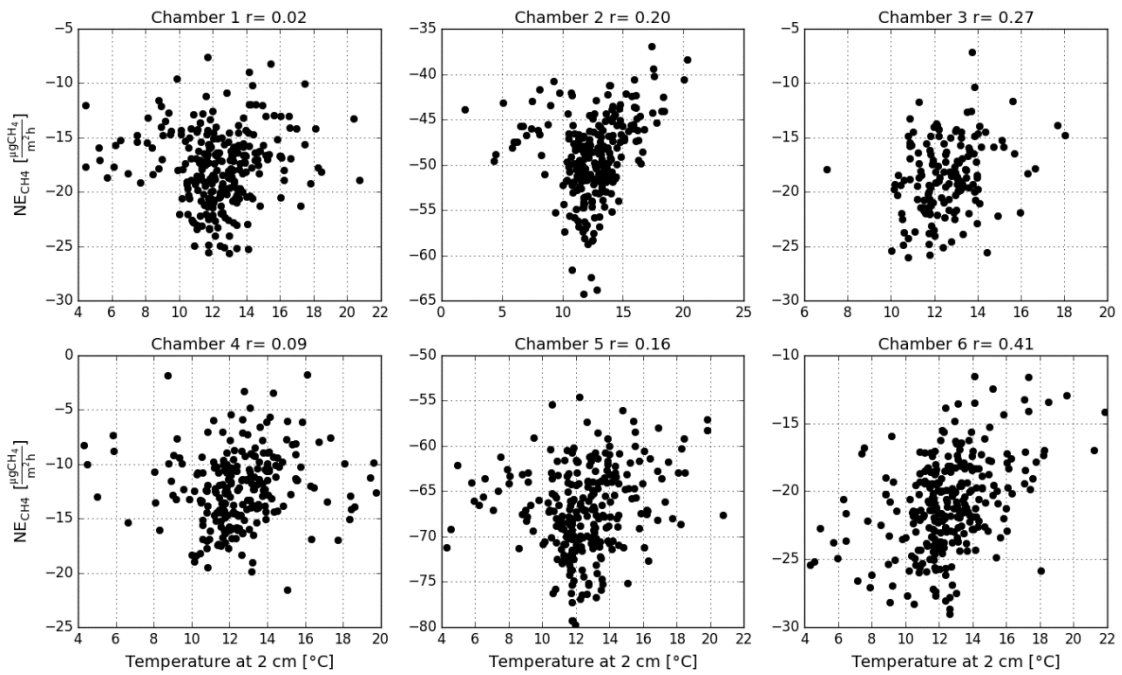

Figure S18. Hourly CH₄ fluxes against the soil temperature at 2 cm depth in 16-30 June 2011. Diurnal variation in CH₄ fluxes was recorded in chamber #6. r in the title shows the Pearson correlation for the data.
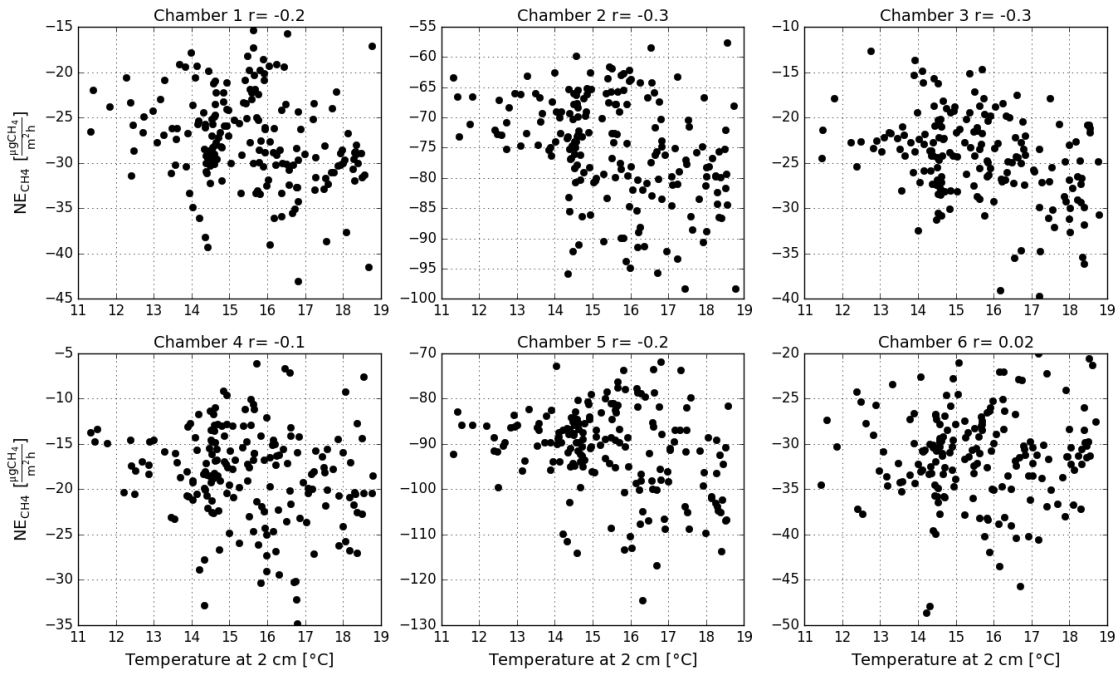
Figure S19. Hourly CH₄ fluxes against the soil temperature at 2 cm depth in 1-15 July 2011. No significant diurnal variation in CH₄ fluxes was recorded. r in the title shows the Pearson correlation for the data.
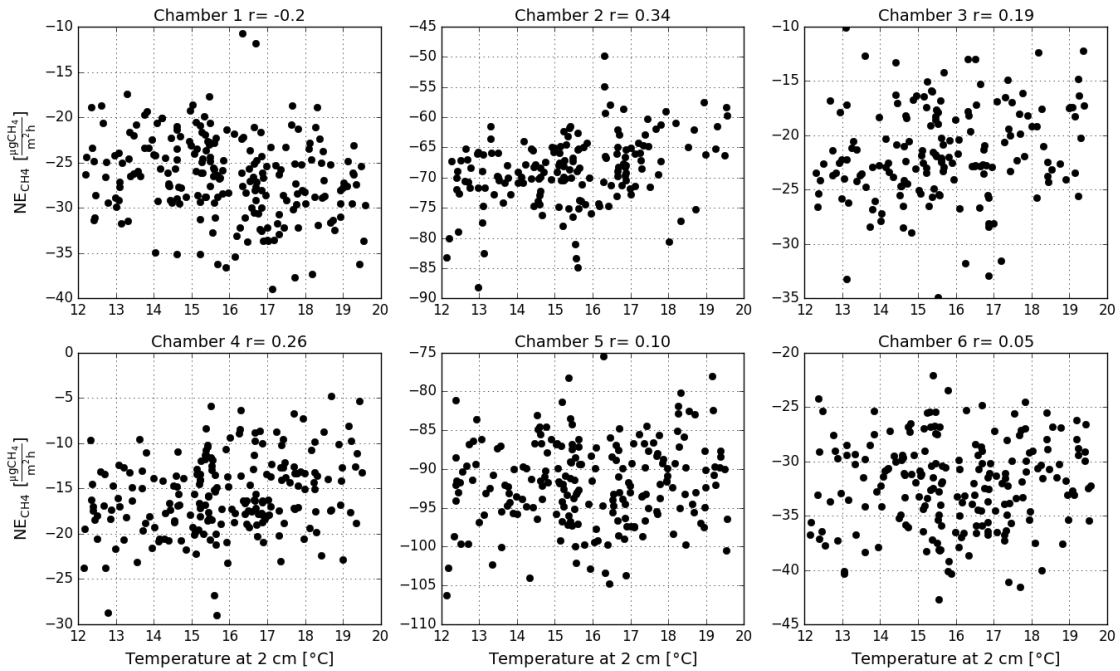

Figure S20. Hourly CH₄ fluxes against the soil temperature at 2 cm depth in 16-31 July 2011. Diurnal variation in CH₄ fluxes was recorded in chambers #2 and #6. r in the title shows the Pearson correlation for the data.
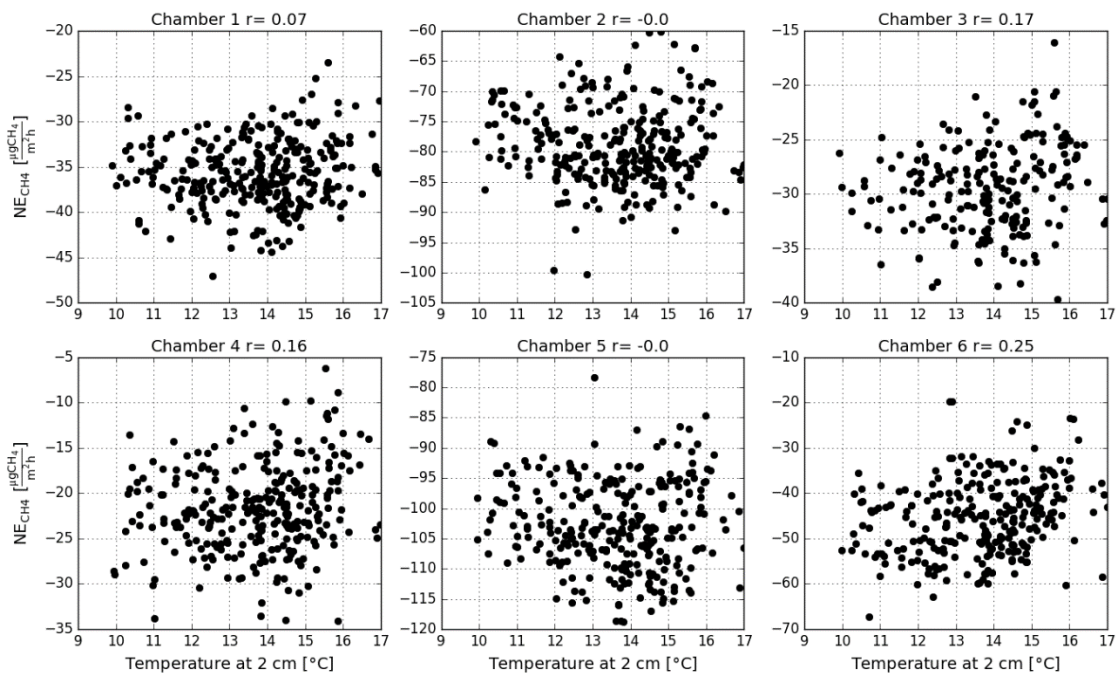
Figure S21. Hourly CH₄ fluxes against the soil temperature at 2 cm depth in 1-15 August 2011. Diurnal variation in CH₄ fluxes was recorded in chamber #2. r in the title shows the Pearson correlation for the data.
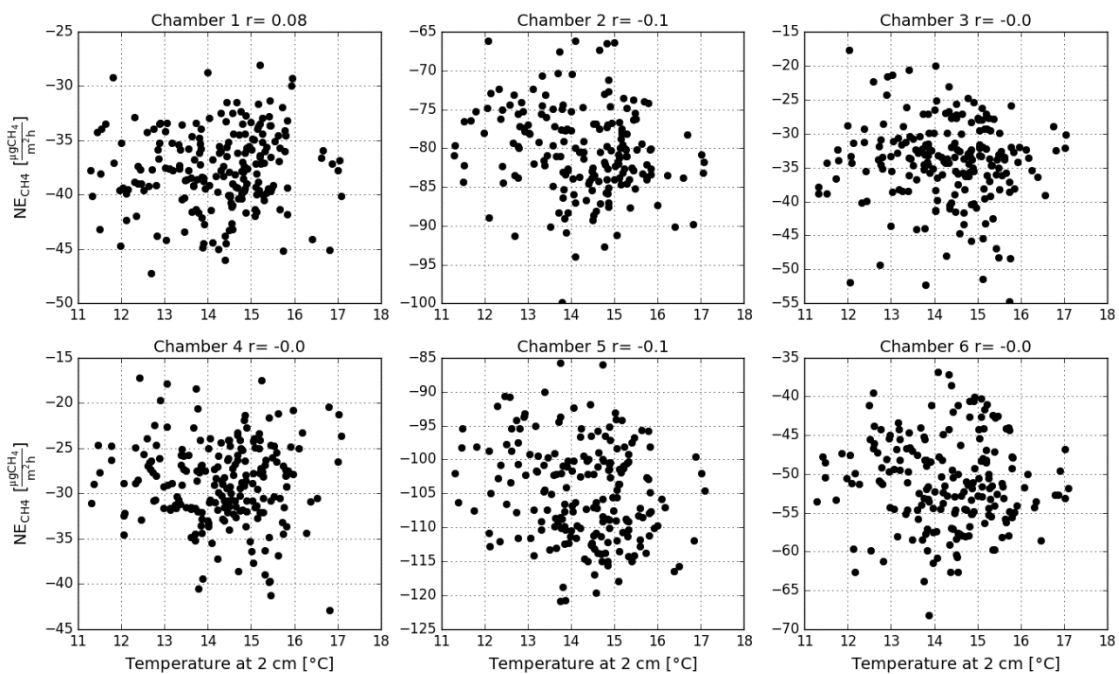

Figure S22. Hourly CH₄ fluxes against the soil temperature at 2 cm depth in 15-31 August 2011. Diurnal variation in CH₄ fluxes was recorded in chamber #1. r in the title shows the Pearson correlation for the data.
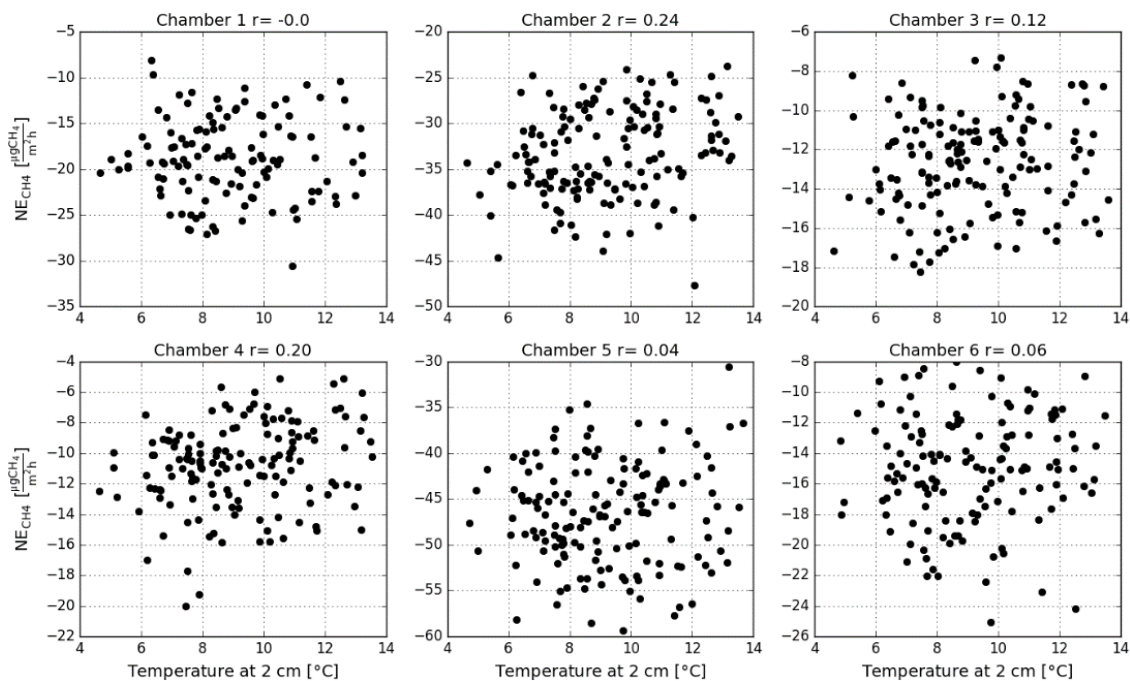
Figure S23. Hourly CH₄ fluxes against the soil temperature at 2 cm depth in 1-15 June 2012. Diurnal variation in CH₄ fluxes was recorded in all the chambers. r in the title shows the Pearson correlation for the data.
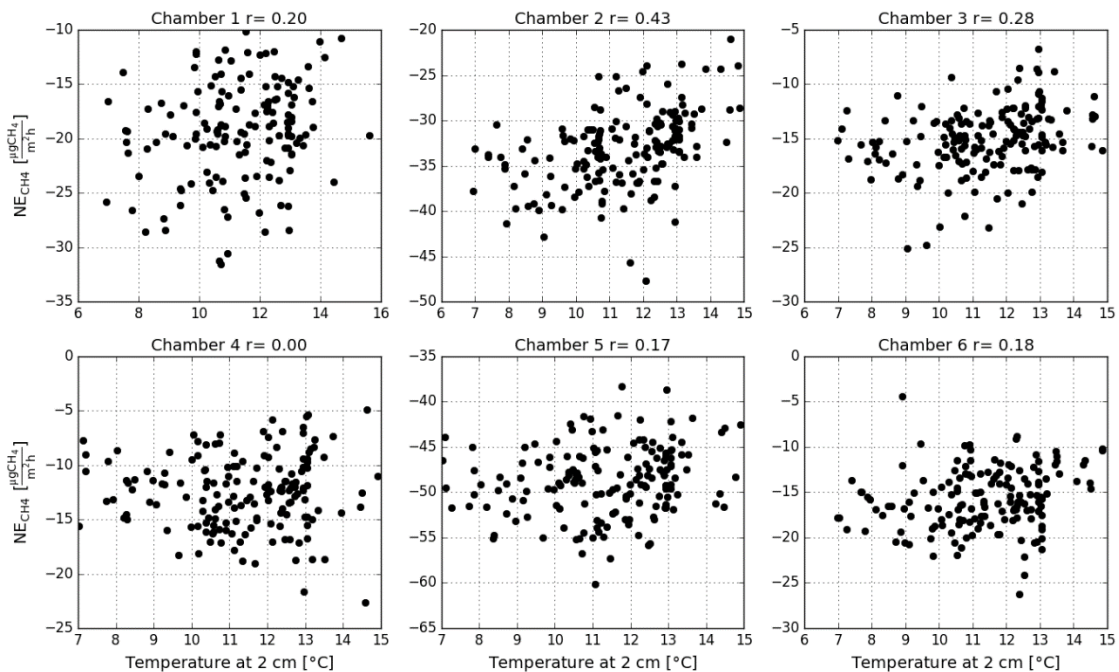

Figure S24. Hourly CH₄ fluxes against the soil temperature at 2 cm depth in 15-30 June 2012. Diurnal variation in CH₄ fluxes was recorded in chamber #2. r in the title shows the Pearson correlation for the data.
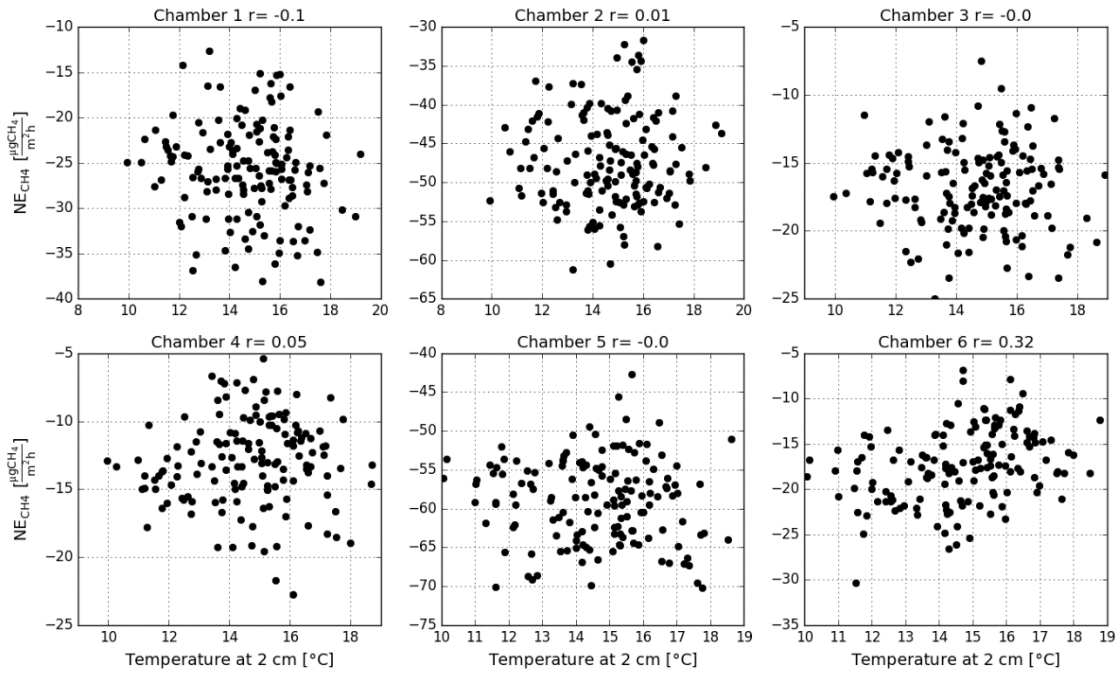
Figure S25. Hourly CH₄ fluxes against the soil temperature at 2 cm depth in 1-15 July 2012. Diurnal variation in CH₄ fluxes was recorded in chambers #2 and #6. r in the title shows the Pearson correlation for the data.
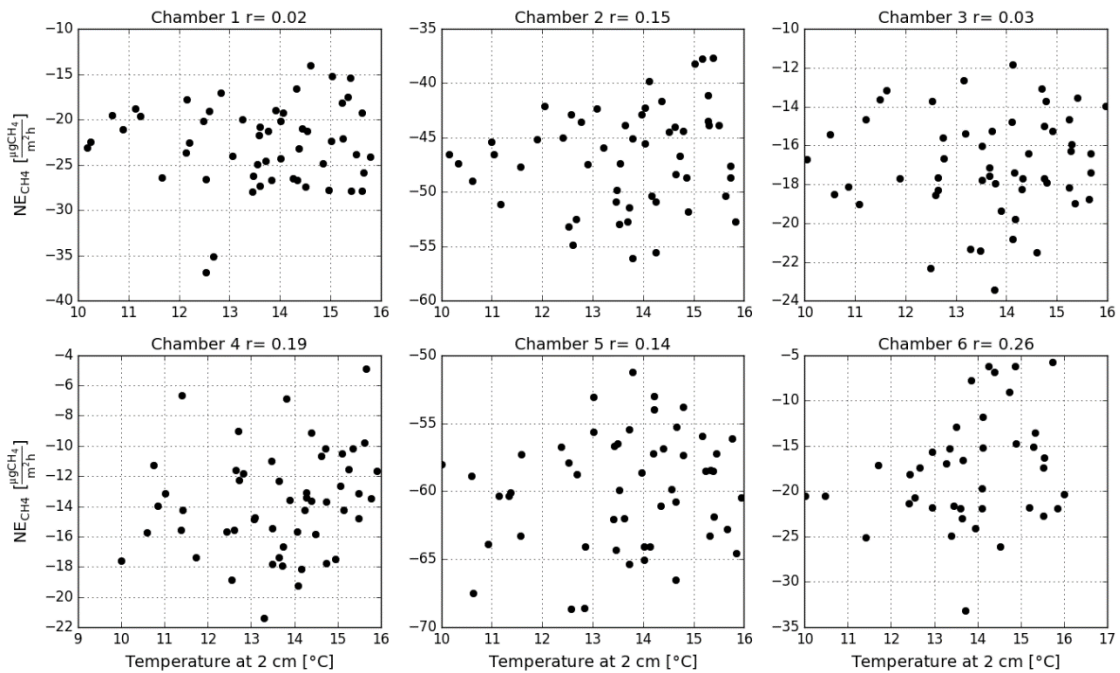

Figure S26. Hourly CH₄ fluxes against the soil temperature at 2 cm depth in 16-31 July 2012. No significant diurnal variation in CH₄ fluxes was recorded. r in the title shows the Pearson correlation for the data.
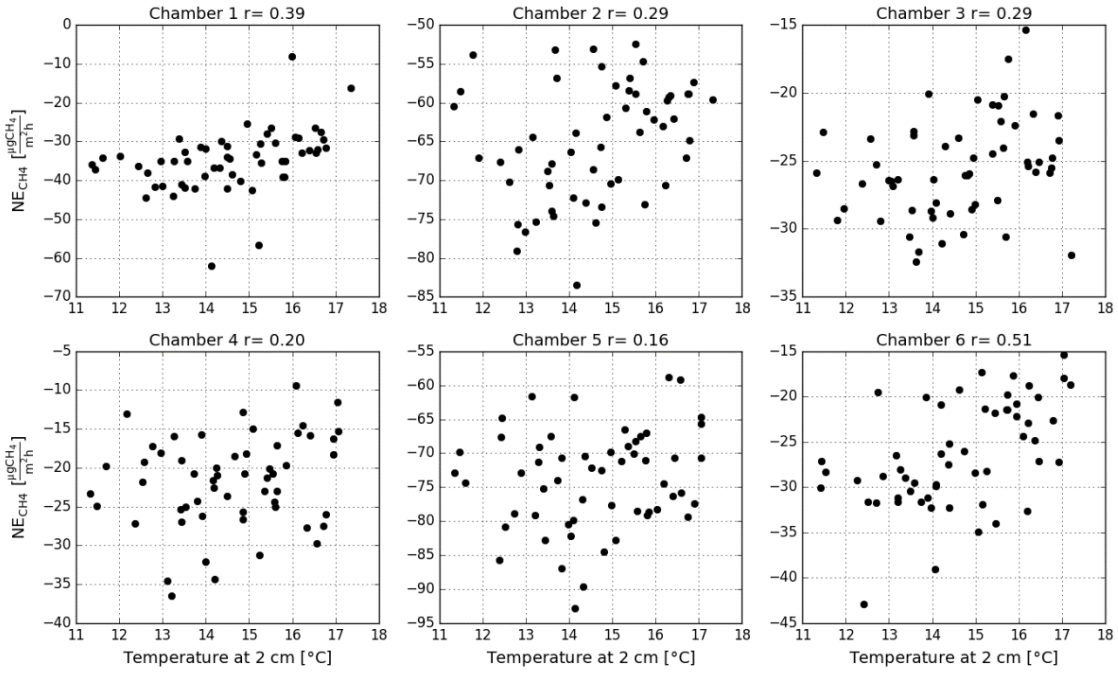
Figure S27. Hourly CH₄ fluxes against the soil temperature at 2 cm depth in 1-15 August 2012. No significant diurnal variation in CH₄ fluxes was recorded. r in the title shows the Pearson correlation for the data.
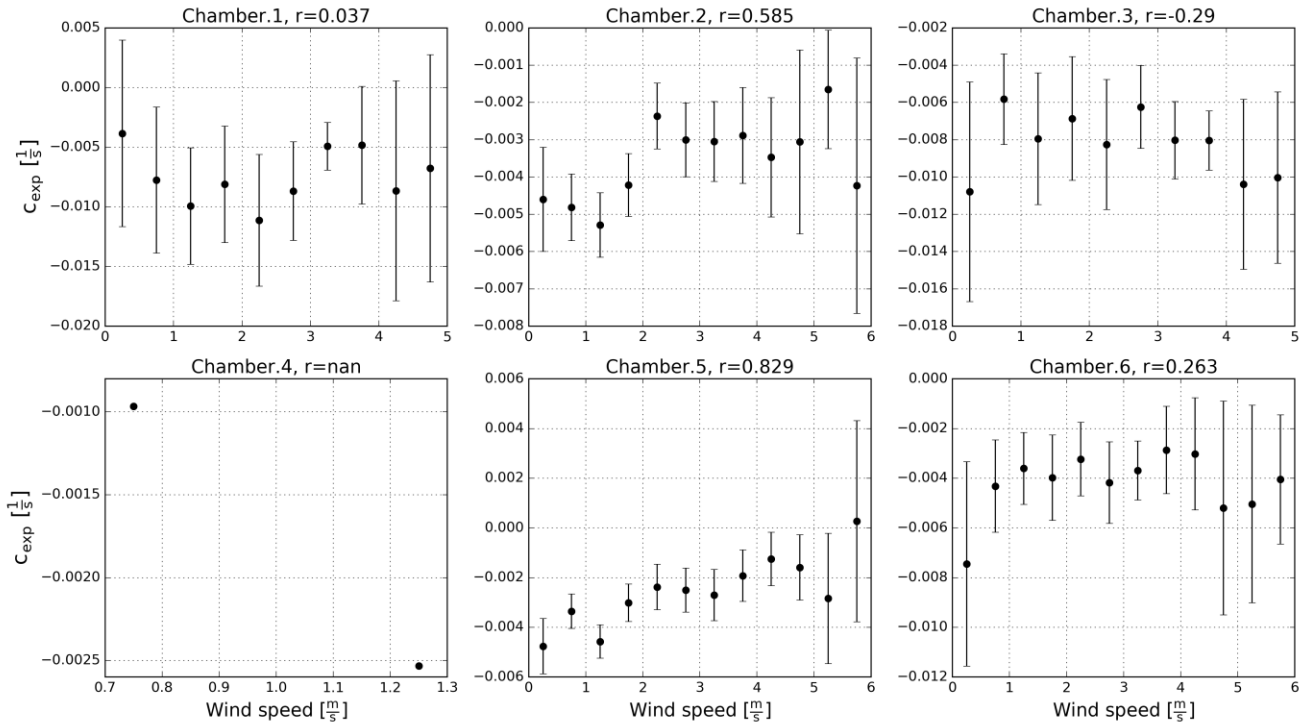

Figure S28. Bin averages of the curvature parameter (c_exp) against wind speed in April 2011. Only negative fluxes (uptake by soil) are included. The error bars show 95 % confidence intervals. r in the title shows the Pearson correlation for the data.

Figure S29. Bin averages of the curvature parameter (c_{exp}) against wind speed in June 2011. Only negative fluxes (uptake by soil) are included. The error bars show 95 % confidence intervals. r in the title shows the Pearson correlation for the data.
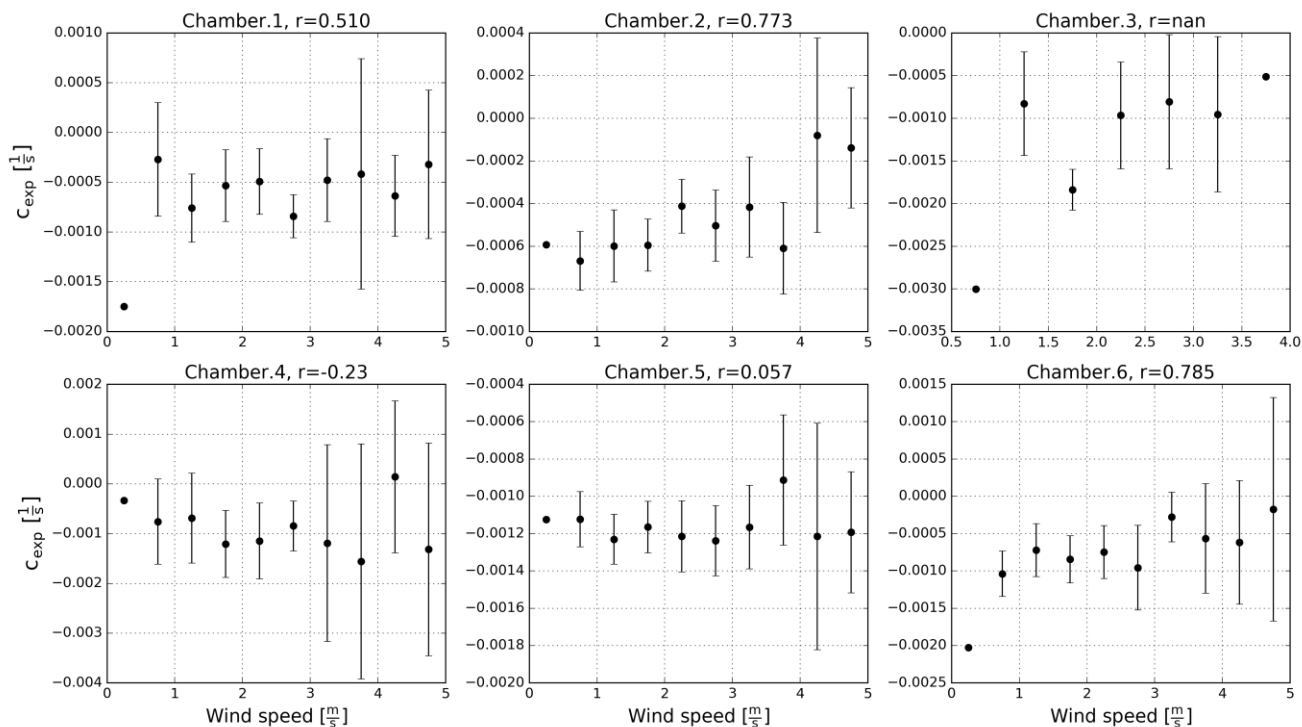

Figure S30. Bin averages of the curvature parameter (c_{exp}) against wind speed in July 2011. Only negative fluxes (uptake by soil) are included. The error bars show 95 % confidence intervals. r in the title shows the Pearson correlation for the data.
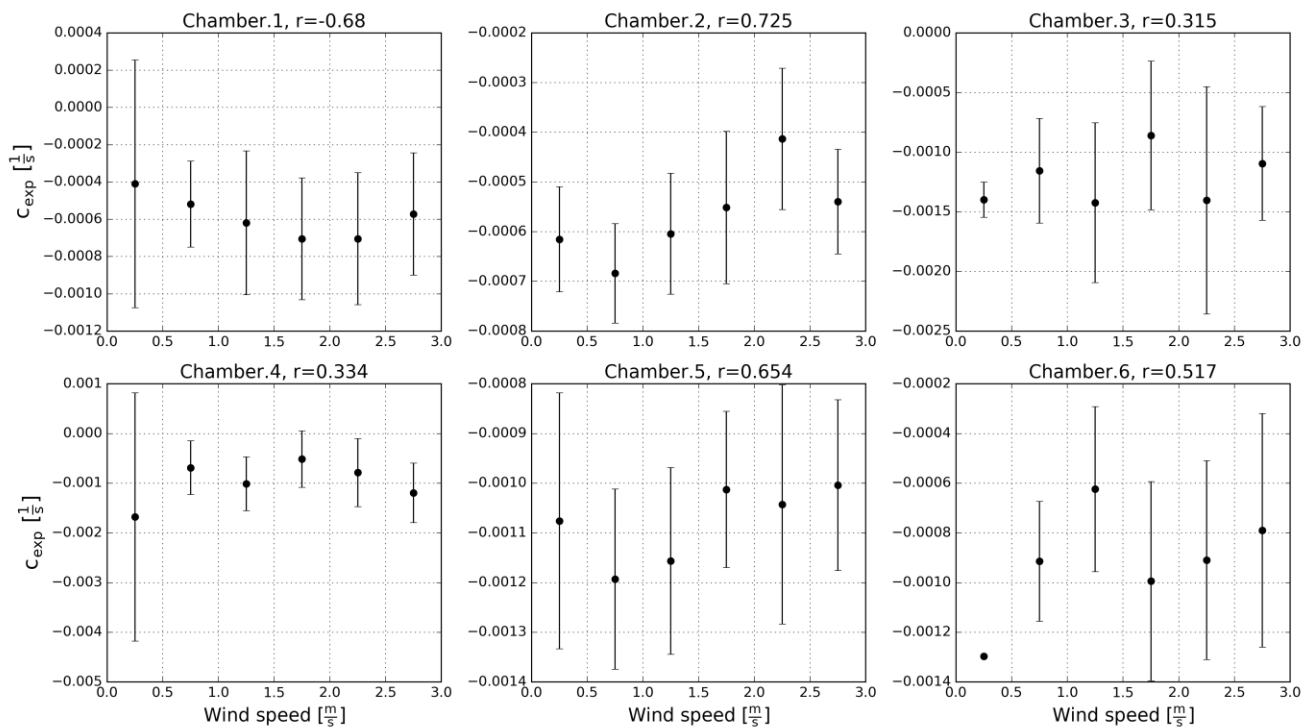
Figure S31. Bin averages of the curvature parameter (c_{exp}) against wind speed in summer (JJA) 2011. Only negative fluxes (uptake by soil) are included. The error bars show 95 % confidence intervals. r in the title shows the Pearson correlation for the data.
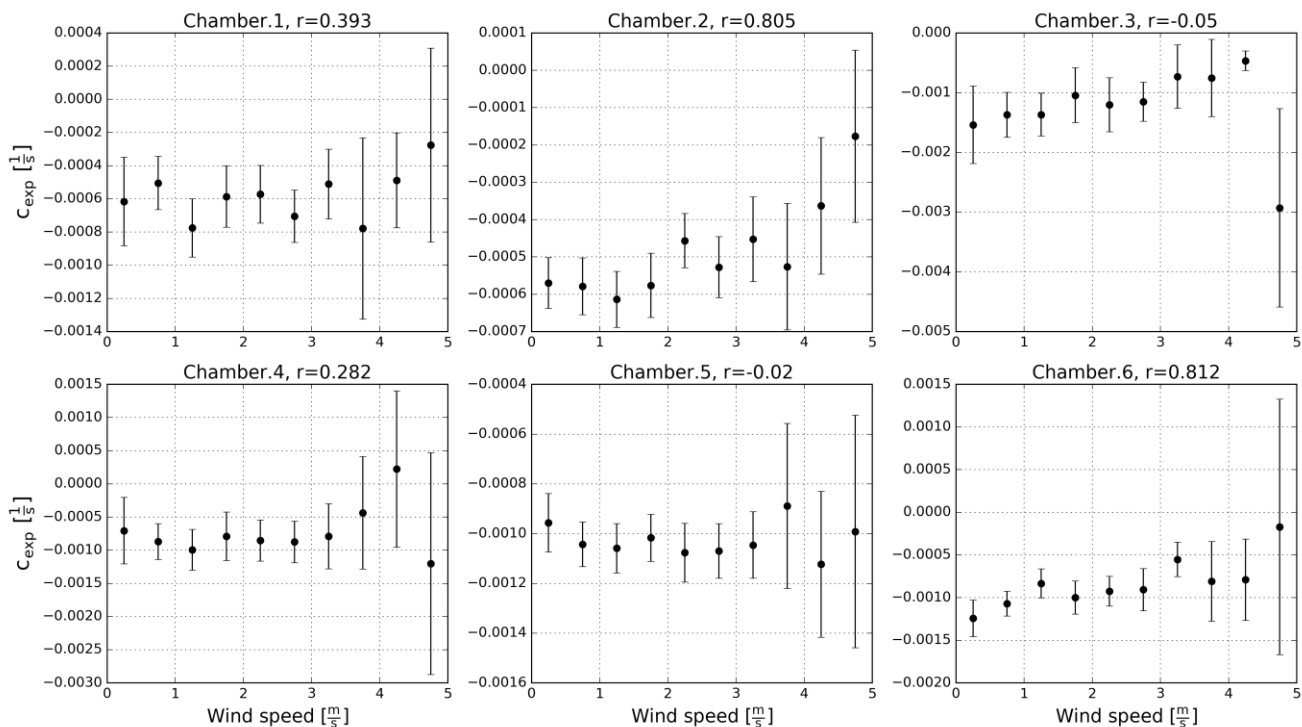

Figure S32. Bin averages of the curvature parameter (c_{exp}) against wind speed in September 2011. Only negative fluxes (uptake by soil) are included. The error bars show 95 % confidence intervals. r in the title shows the pearson correlation for the data.
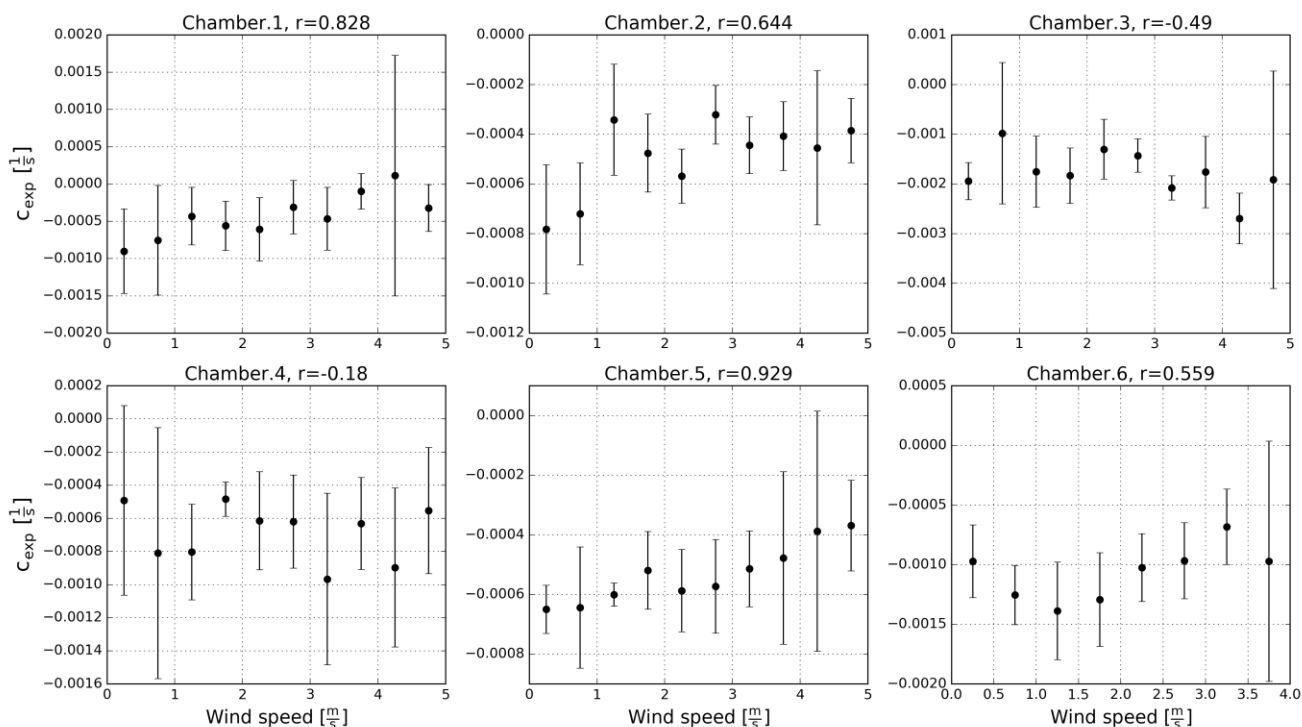
Figure S33. Bin averages of the curvature parameter (c_{exp}) against wind speed in autumn (SON) 2011. Only negative fluxes (uptake by soil) are included. The error bars show 95 % confidence intervals. r in the title shows the Pearson correlation for the data.
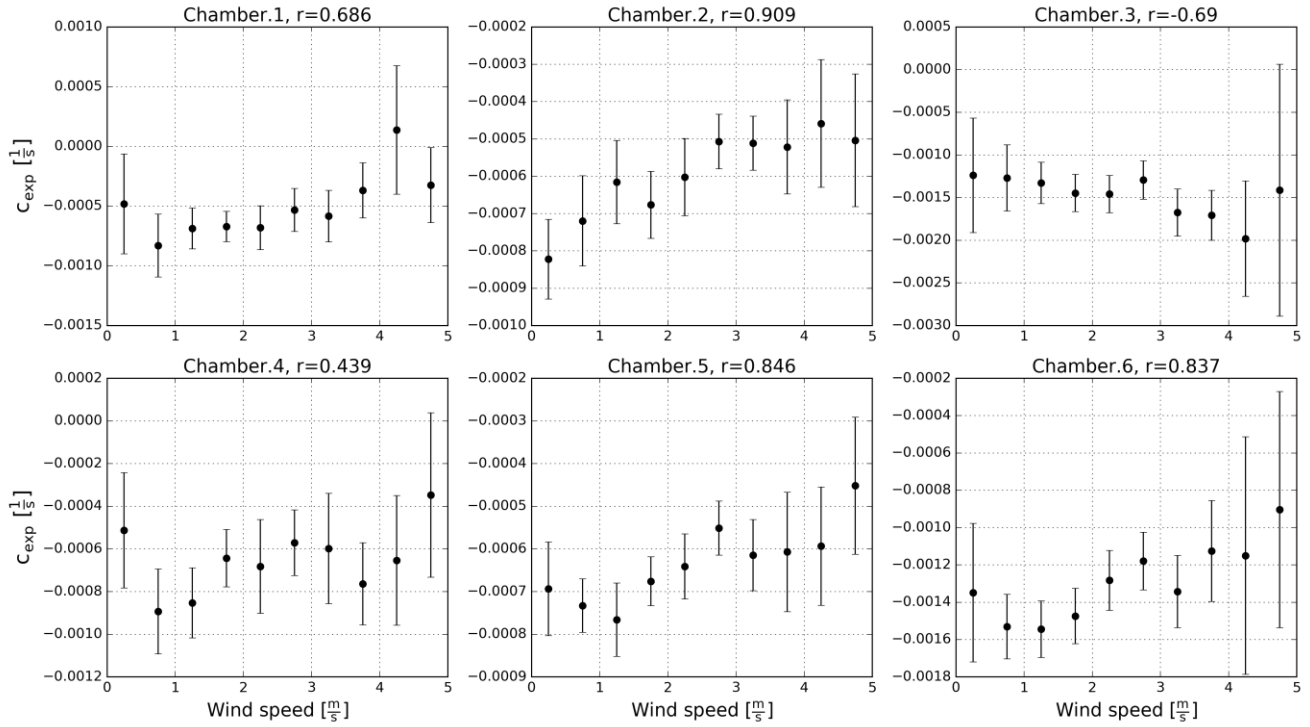

Figure S34. Bin averages of the curvature parameter (c_{exp}) against wind speed in winter (DJF) 2011-2012. Only negative fluxes (uptake by soil) are included. The error bars show 95 % confidence intervals. r in the title shows the Pearson correlation for the data.
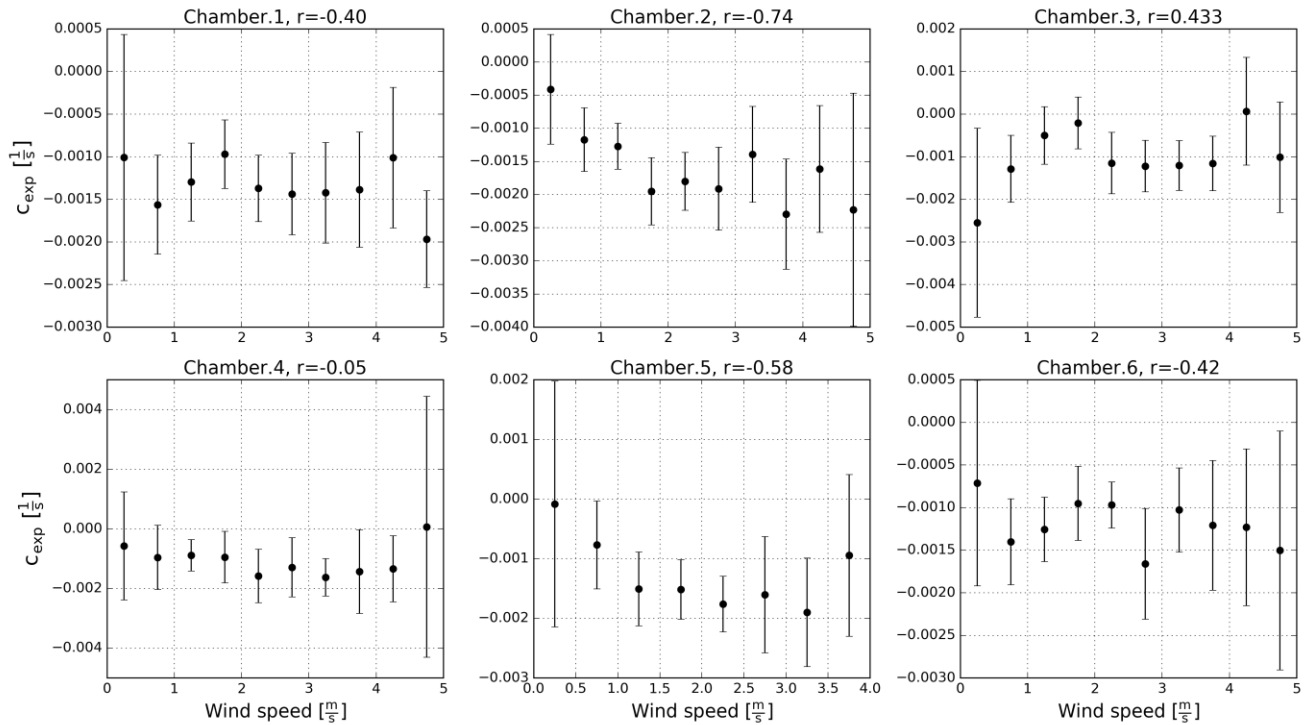
Figure S35. Bin averages of the curvature parameter (c_{exp}) against wind speed in May 2012. Only negative fluxes (uptake by soil) are included. The error bars show 95 % confidence intervals. r in the title shows the Pearson correlation for the data.
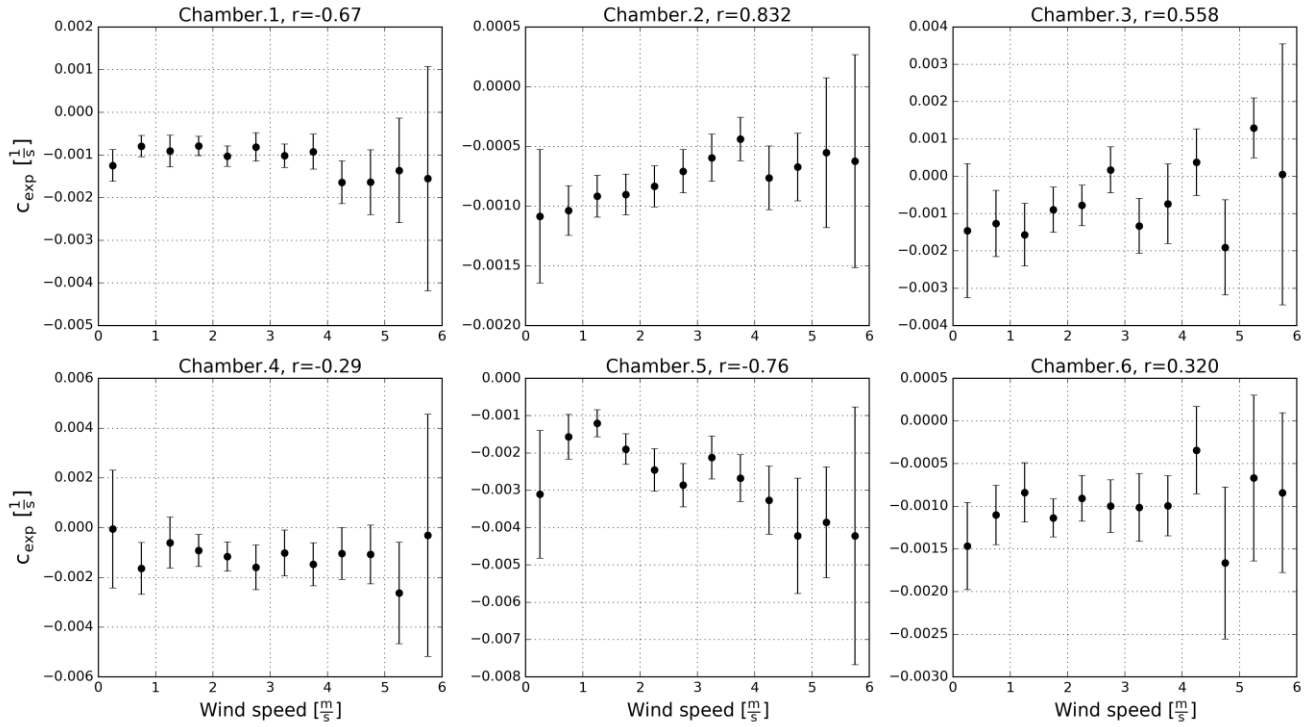

Figure S36. Bin averages of the curvature parameter (c_{exp}) against wind speed in July 2012. Only negative fluxes (uptake by soil) are included. The error bars show 95 % confidence intervals. r in the title shows the Pearson correlation for the data.
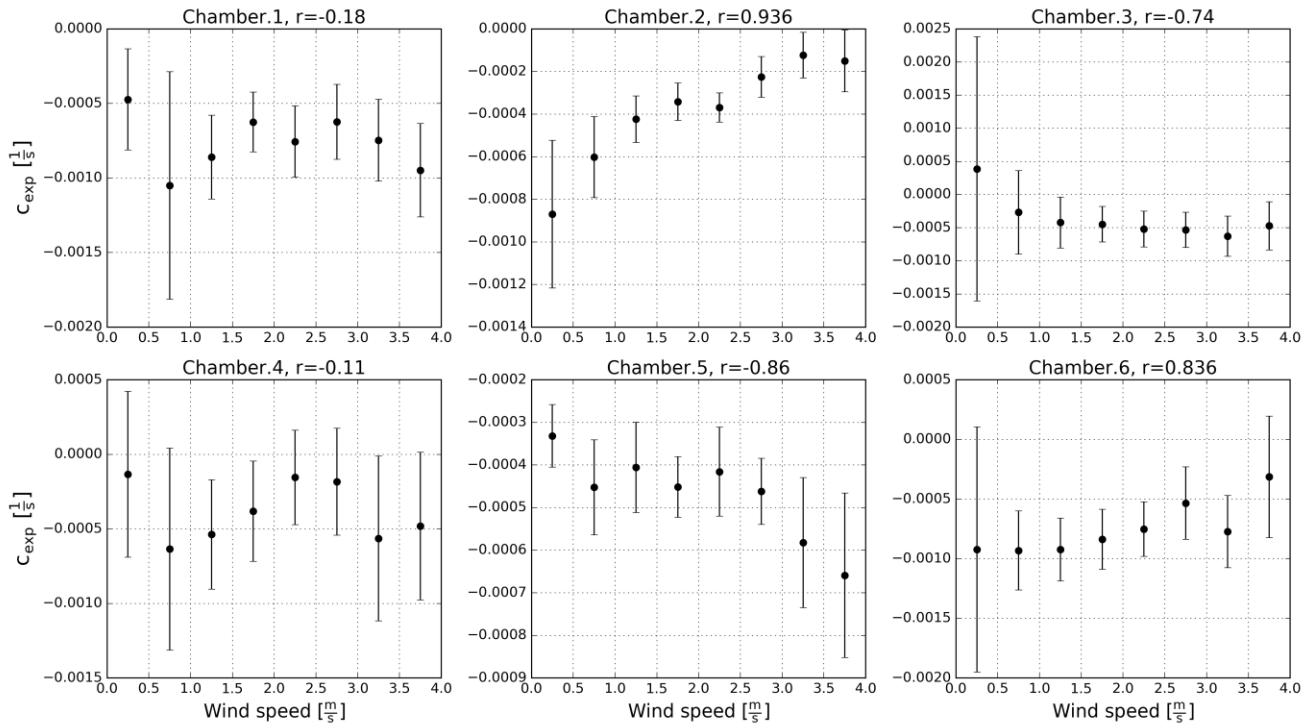
Figure S37. Bin averages of the curvature parameter (c_{exp}) against wind speed in summer (JJA) 2012. Only negative fluxes (uptake by soil) are included. The error bars show 95 % confidence intervals. r in the title shows the pearson correlation for the data.
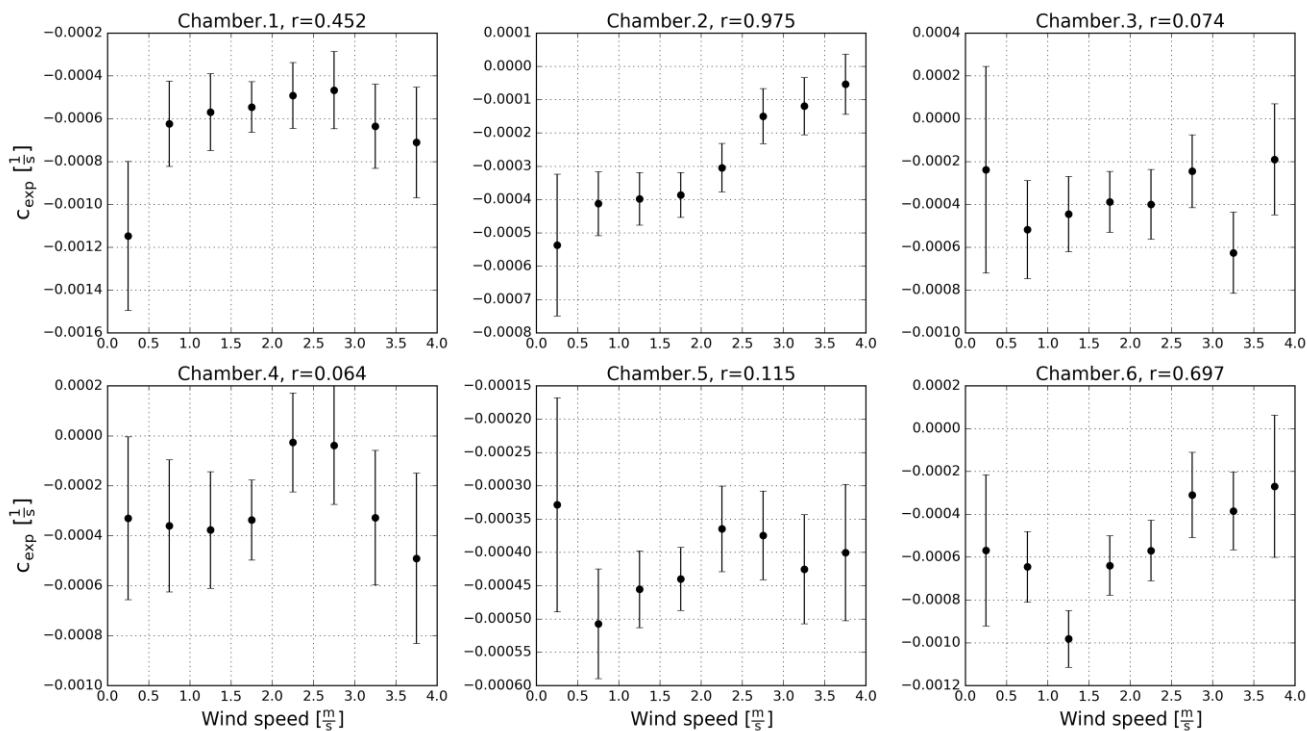

Figure S38. Bin averages of the curvature parameter (c_{exp}) against wind speed in September 2012. Only negative fluxes (uptake by soil) are included. The error bars show 95 % confidence intervals. r in the title shows the pearson correlation for the data
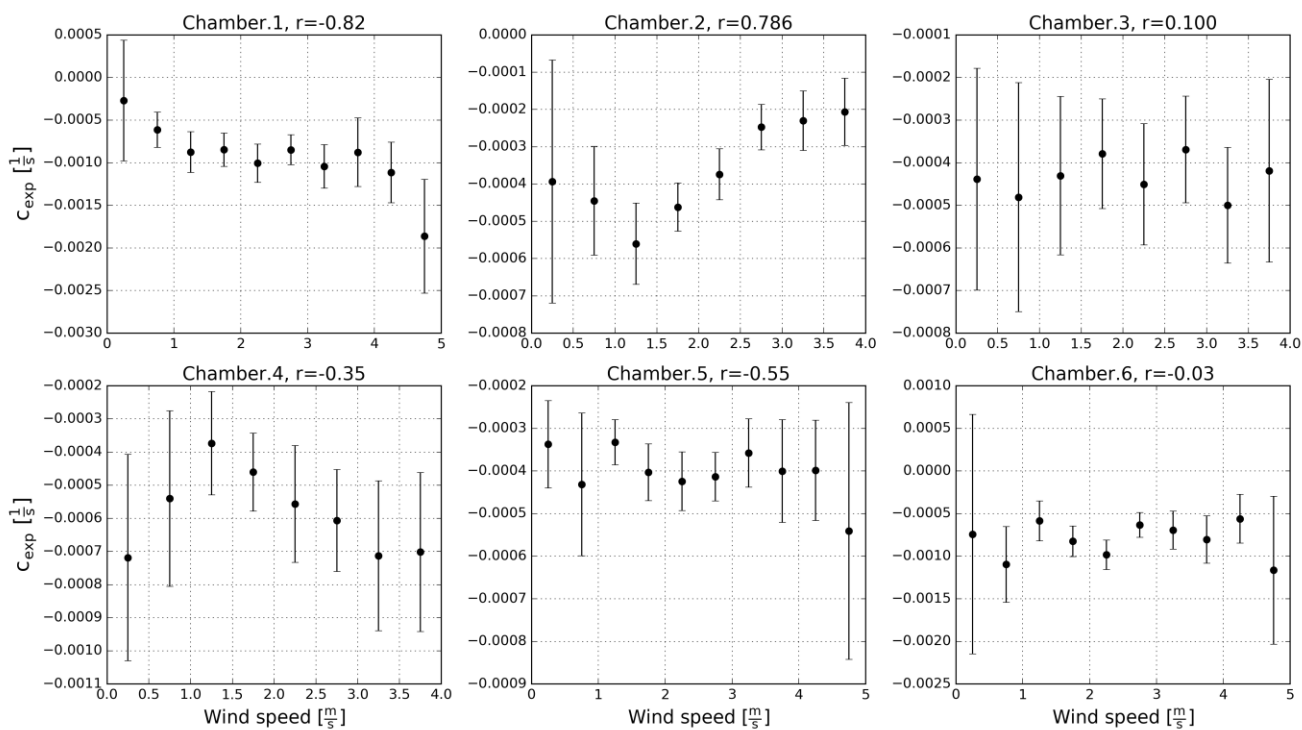
Figure S39. Bin averages of the curvature parameter (c_{exp}) against wind speed in October 2012. Only negative fluxes (uptake by soil) are included. The error bars show 95 % confidence intervals. r in the title shows the pearson correlation for the data.
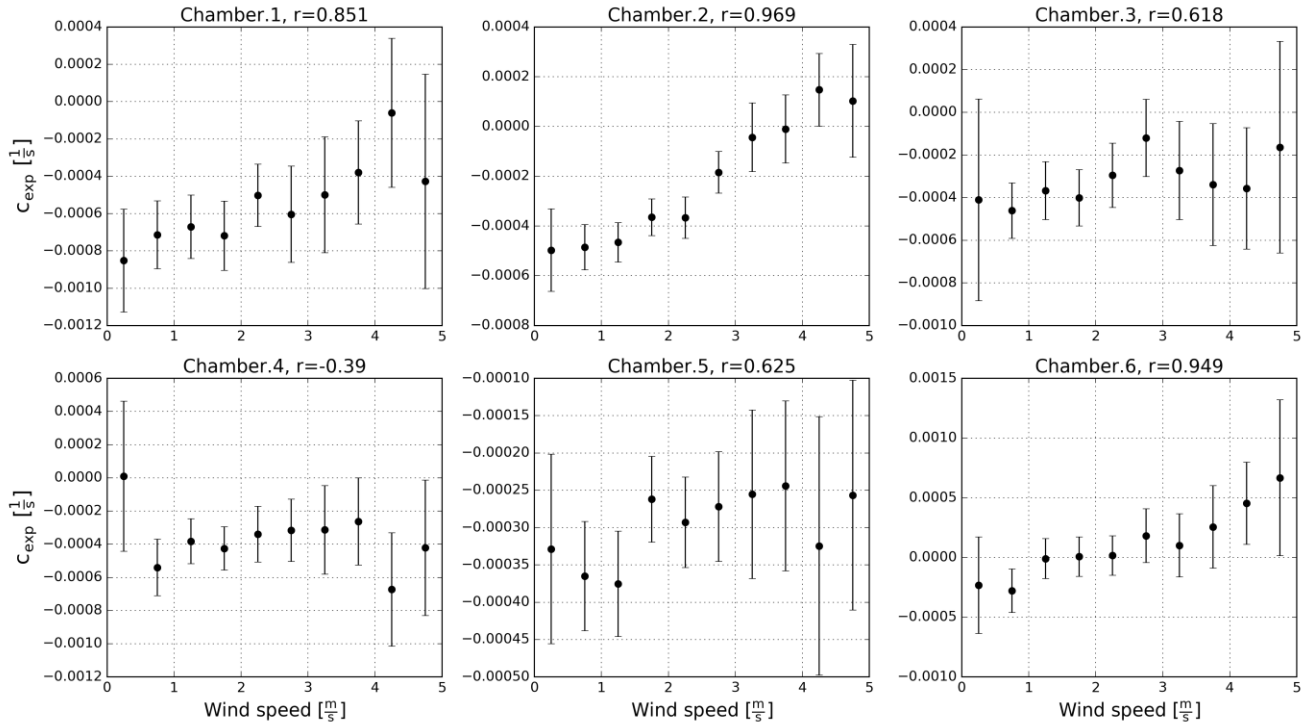

Figure S40. Bin averages of the curvature parameter (c_{exp}) against wind speed in February 2013. Only negative fluxes

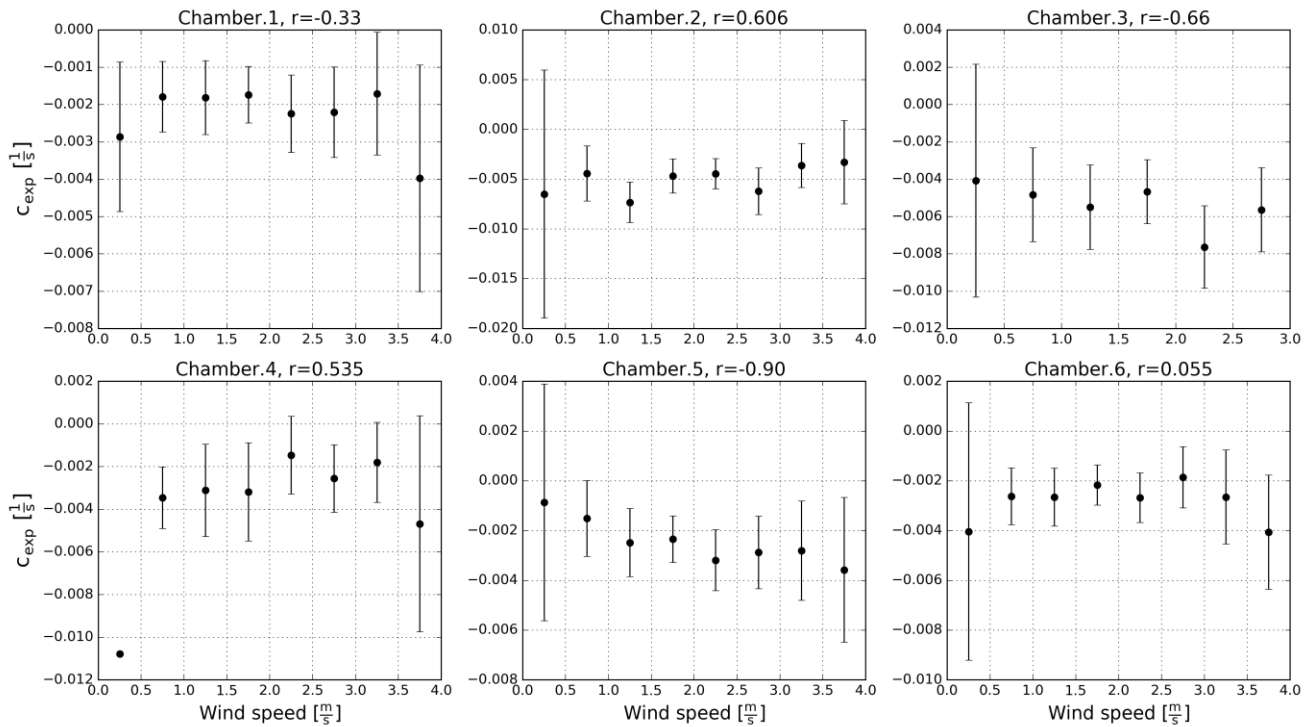(uptake by soil) are included. The error bars show 95 % confidence intervals. r in the title shows the pearson correlation for the data.